

## Supporting Information

### **Molten-salt assisting synthesis of high-performance oxide cathode for the sodium-ion battery: Na<sub>0.44</sub>MnO<sub>2</sub> as a case**

Haijun Zhao,<sup>a</sup> Linrong Wu,<sup>a</sup> Jinlv Tian,<sup>a</sup> Ding Zhang,<sup>\*a, b</sup> Xiaofeng Li,<sup>\*a</sup> Shoudong Xu,<sup>a</sup> Liang Chen,<sup>a</sup> Qun Yi,<sup>b</sup> Kehua Dai<sup>\*c</sup> and Huijuan Guo<sup>b</sup>

- a. College of Chemical Engineering and Technology, Taiyuan University of Technology, Taiyuan 030024, China.
- b. School of Chemical Engineering and Pharmacy, Wuhan Institute of Technology, Wuhan, 430205, China.
- c. College of Chemistry, Tianjin Normal University, Tianjin 300387, China.

**Submitted in *New Journal of Chemistry***

### ***Synthesis of cathode materials:***

$\text{Na}_{0.44}\text{MnO}_2$  synthesized by molten salt method with different molten salt systems. Using absolute ethanol as the dispersant,  $\text{Mn}_2\text{O}_3$ ,  $\text{Na}_2\text{CO}_3$ , and NaCl/KCl (molar ratio 1:1), in a molar ratio of 1:0.44:20, were uniformly grounded for 1 hour in an agate mortar. Then they were calcined in a muffle furnace at 700°C, 750°C, and 800°C for 2 h in an air atmosphere. Finally, the NaCl and KCl was removed by washing the mixture with deionized water, and the obtained filter cake was dried in an oven at 60°C to obtain the  $\text{Na}_{0.44}\text{MnO}_2$ . Moreover, they are recorded as NaCl+KCl-700, NaCl+KCl-750 and NaCl+KCl-800, respectively.

$\text{Na}_{0.44}\text{MnO}_2$  synthesized by molten salt method with different manganese sources. Using absolute ethanol as the dispersant, the manganese source ( $\text{MnO}$ ,  $\text{Mn}_2\text{O}_3$  and  $\text{MnO}_2$ ),  $\text{Na}_2\text{CO}_3$ , and NaCl, in a molar ratio (Na:Mn) of 1:0.44:20, were uniformly grounded for 1 hour in an agate mortar. Then they were calcined in a muffle furnace at 800°C for 2 h in an air atmosphere. Finally, the NaCl was removed by washing the mixture with deionized water, and the obtained filter cake was dried in an oven at 60°C to obtain the  $\text{Na}_{0.44}\text{MnO}_2$ . Moreover, they are denoted as NMO-MnO, NMO- $\text{Mn}_2\text{O}_3$  and NMO- $\text{MnO}_2$ , respectively.

**Note:** In this work, NMO-8002, NaCl-800 and NMO- $\text{Mn}_2\text{O}_3$  are the same material, but the code names are different for the convenience of comparing the properties with other materials.

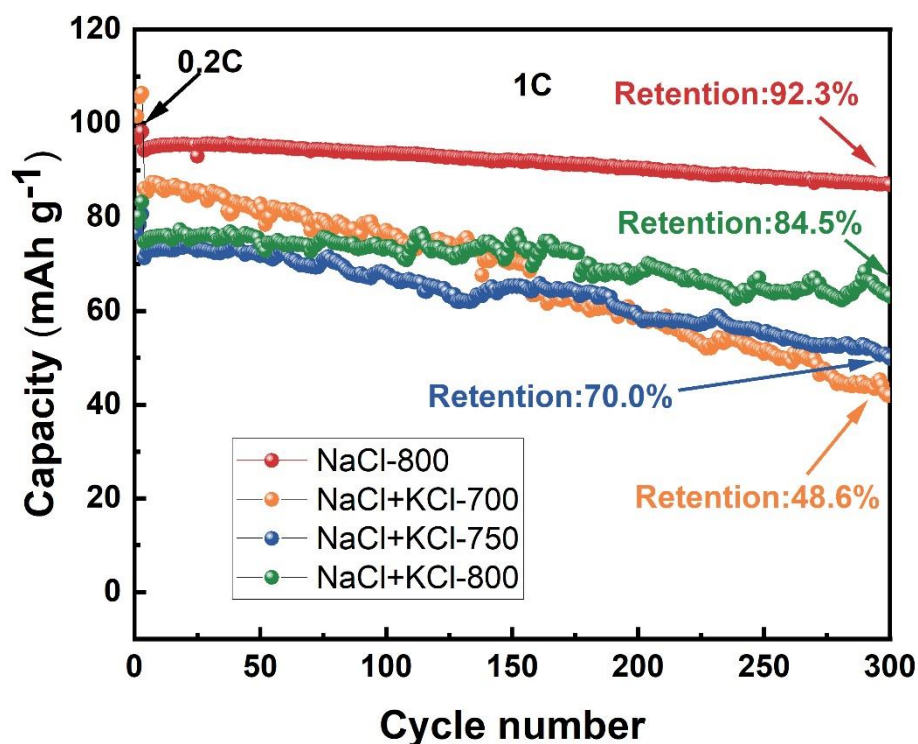


**Figure S1. Long-cycle performance of NMO synthesized from different molten salt systems**

It can be seen the long-cycle performance of  $\text{Na}_{0.44}\text{MnO}_2$  synthesized by different molten salt systems at 1 C for 300 cycles (the first three cycles were run at 0.2 C for electrode activation) in Figure S1. The capacity of NaCl-800 decreases from 94.2 mAh g<sup>-1</sup> to 86.9 mAh g<sup>-1</sup>, and the capacity retention rate is 92.3%. However, the capacities of NaCl+KCl-700, NaCl+KCl-750, and NaCl+KCl-800 synthesized by NaCl/KCl (1:1) mixed molten salt system under three different sintering temperatures are 86.1 mAh g<sup>-1</sup>, 71.3 mAh g<sup>-1</sup> and 74.7 mAh g<sup>-1</sup> in the first cycle at 0.2 C, respectively. And the capacity retention rates are 48.6%, 70.0% and 84.5% at 1 C after 300 cycles, respectively. NaCl-800 synthesized with NaCl single molten salt system has the best structural stability at 1 C.

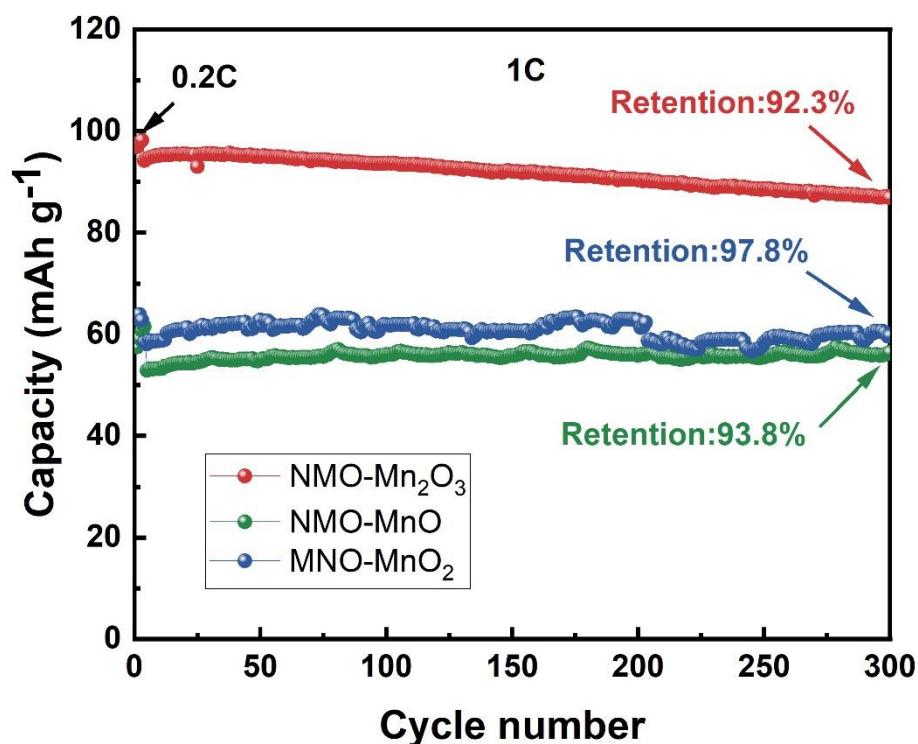


**Figure S2. Long-cycle performance of NMO synthesized from different manganese sources**

Figure S2 shows the long-cycle performance of  $\text{Na}_{0.44}\text{MnO}_2$  synthesized with different manganese sources at 1 C for 300 cycles (the first three cycles were run at 0.2 C for electrode activation). The capacity of  $\text{NMO-Mn}_2\text{O}_3$  decreases from  $94.2 \text{ mAh g}^{-1}$  to  $86.9 \text{ mAh g}^{-1}$ , and the capacity retention rate is 92.3%. In contrast, the capacities of  $\text{NMO-MnO}$  and  $\text{NMO-MnO}_2$  synthesized with two different manganese sources are  $56.4 \text{ mAh g}^{-1}$  and  $59.7 \text{ mAh g}^{-1}$  in the first cycle at 0.2 C, respectively. And their capacity retention rates are 93.8% and 97.8% at 1 C after 300 cycles, respectively. Although the NMO synthesized with MnO and  $\text{MnO}_2$  as the manganese source has slightly better cycle stability, the capacity is not as good as that of the NMO synthesized with  $\text{Mn}_2\text{O}_3$  as the manganese source.

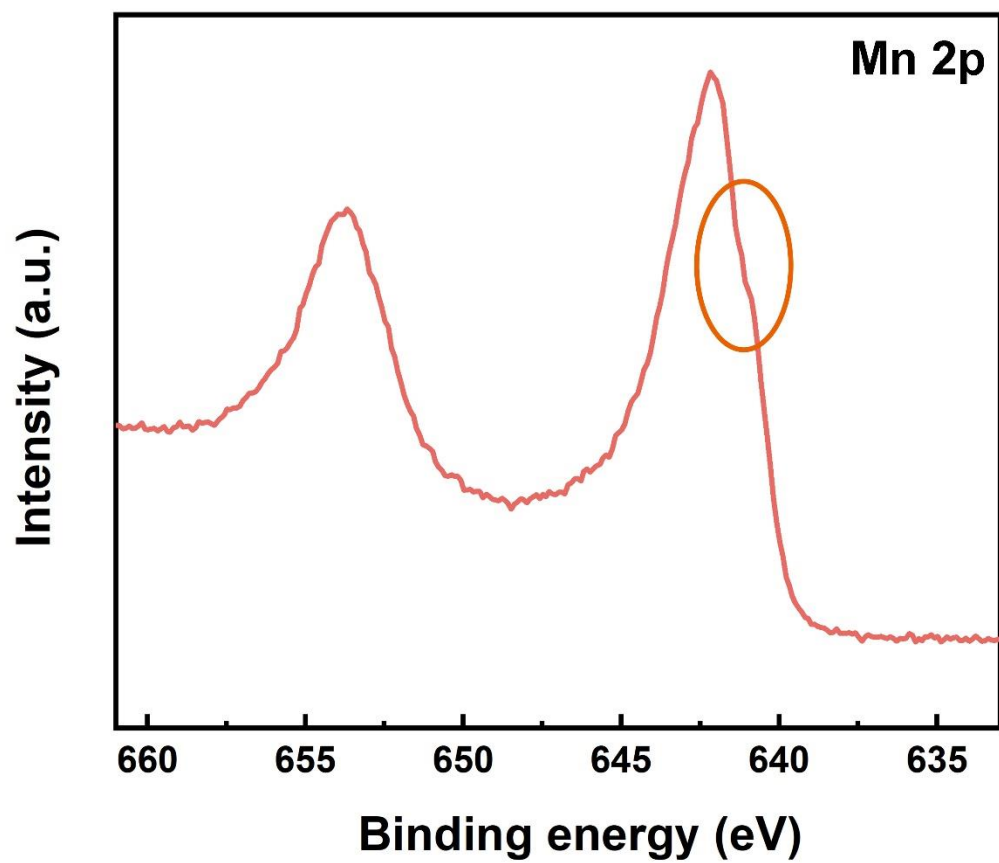


Figure S3. XPS fine spectrum of NMO-8002

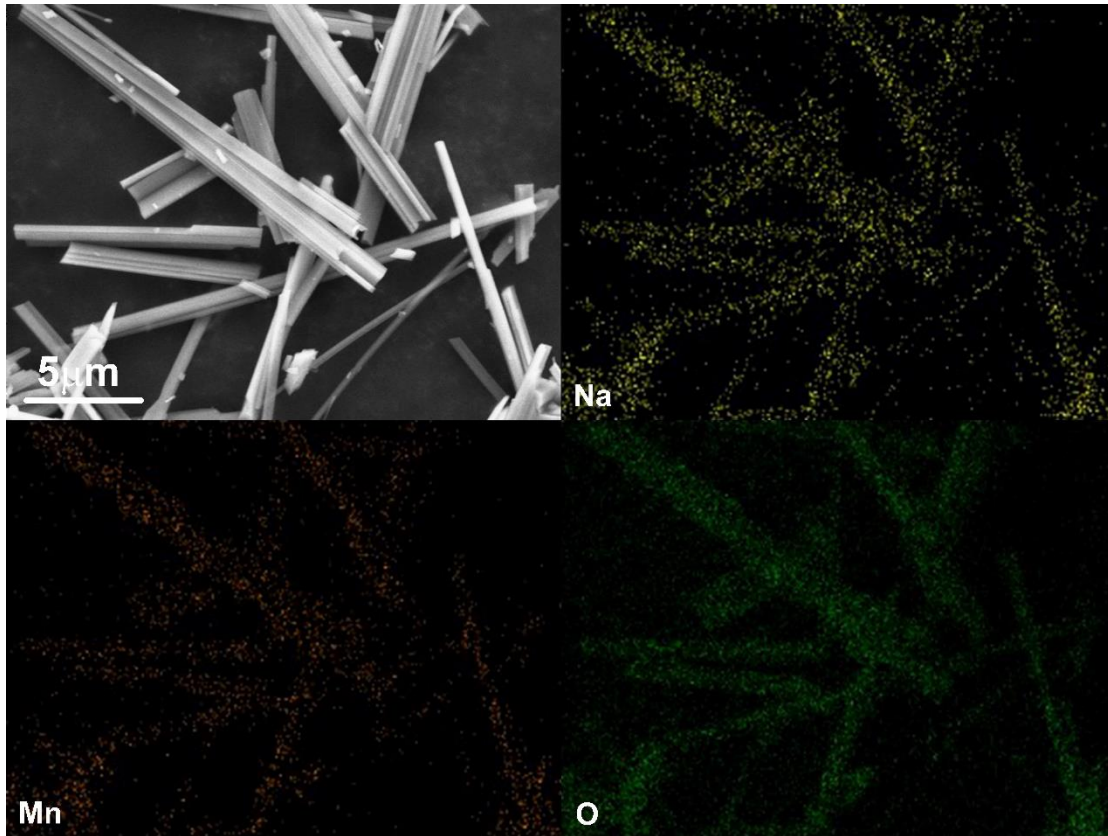


Figure S4. SEM-EDS elemental mapping images of NMO-8002

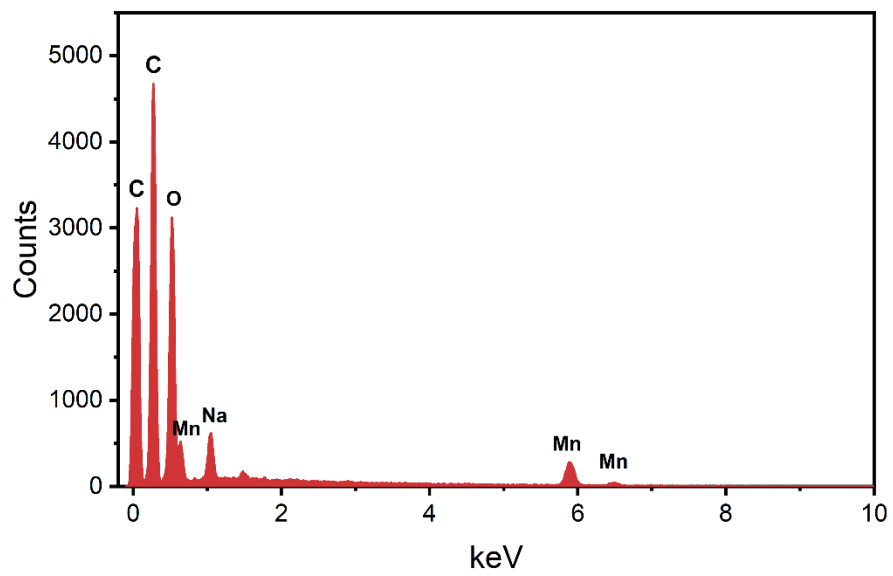


Figure S5. X-ray energy dispersive spectrum of NMO-8002

The calculation of pseudo-capacitance contribution rate

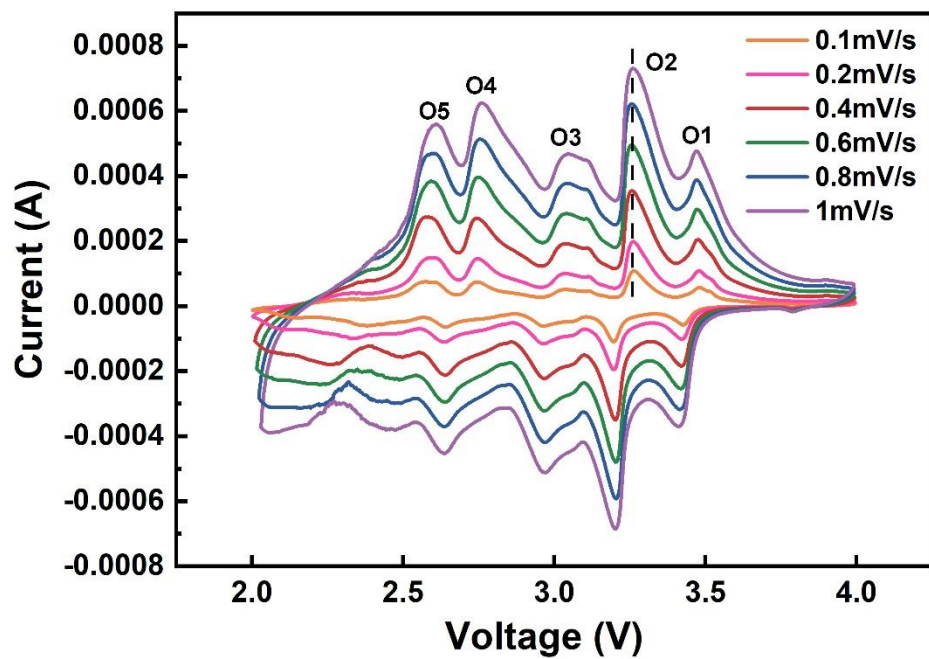


Figure S6. CV curves at different scan rates after depolarization of NMO-8002

In order to judge the behavior of electrode materials, it can be calculated according to Formula S1 and S2:

$$i_p = av^b \quad (\text{Formula S1})$$

$$\lg i_p = \lg a + b \lg v \quad (\text{Formula S2})$$

to judge whether the material is controlled by diffusion, by surface or by combination of diffusion and surface<sup>1,2</sup>. Where  $i_p$  is the peak current in the CV curves,  $v$  is the scan rate, and  $a$  and  $b$  are constants, respectively.

When  $b=0.5$ , the material behaves as diffusion controlled.

When  $b \geq 1$ , the material behaves as surface control.

When  $0.5 < b < 1$ , the material is controlled by combination of diffusion and surface.

In the calculation of the pseudo-capacitance contribution, it can be calculated according to Formula S3 and S4:

$$i(V) = k_1 v + k_2 v^{0.5} \quad (\text{Formula S3})$$

$$i(V)/v^{0.5} = k_1 v^{0.5} + k_2 \quad (\text{Formula S4})$$

Where  $i(V)$  is the peak current,  $v$  is the scan rate, and  $k_1$  and  $k_2$  are both constants. In Formula S3,  $k_1 v$  is the contribution of surface-controlled reactions to the current, and  $k_2 v^{0.5}$  is the contribution of diffusion-controlled reactions.



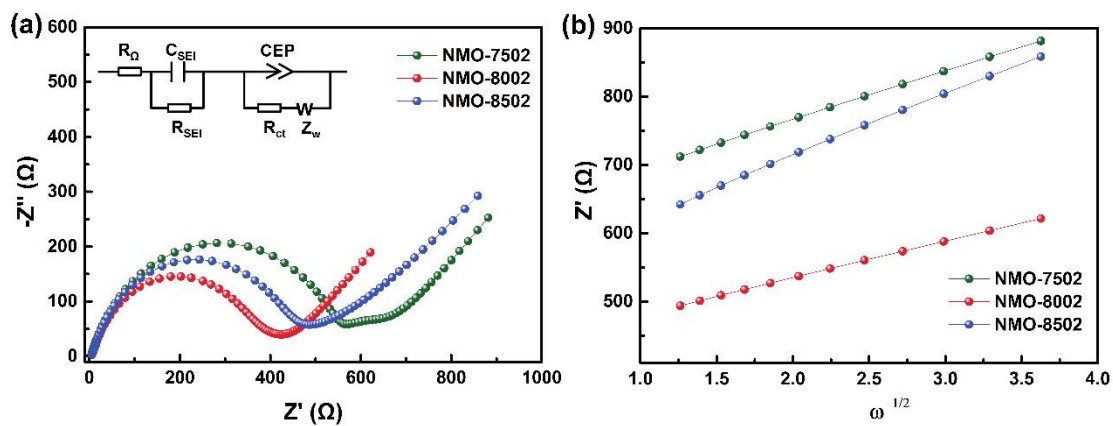


Figure S7. (a)EIS plots after rate test at 2.25 V; (b) the relationship between  $Z'$  and  $\omega^{1/2}$  in the low-frequency region figure;

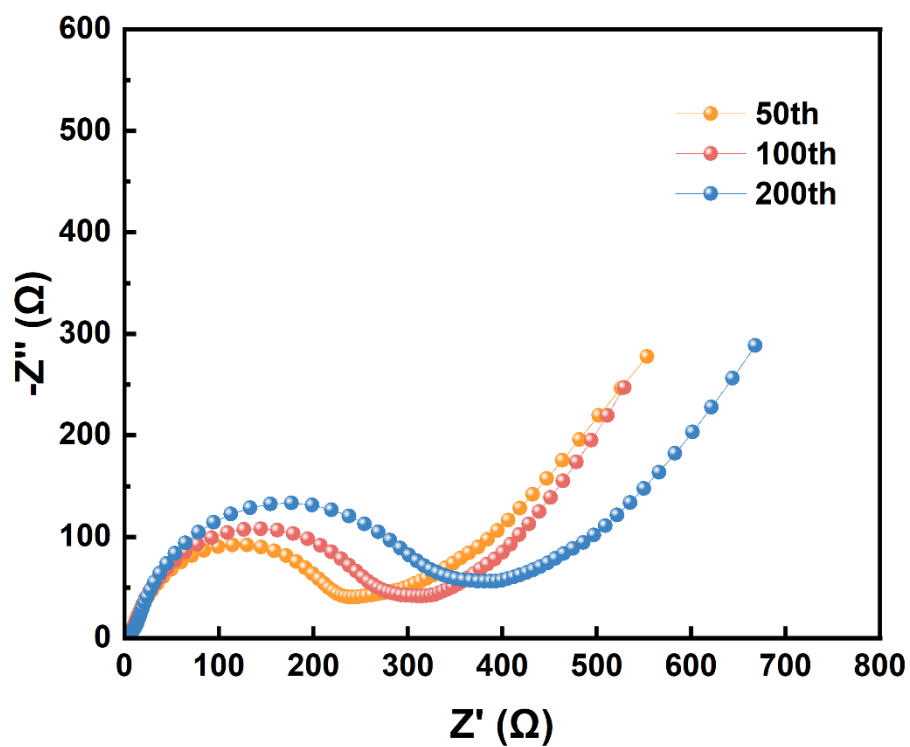


Figure S8. EIS plots of NMO-8002 after the 50th, 100th and 200th cycles at 5C at 2.4 V

**The amount of NaCl molten salt does not affect the growth mechanism of NMO.**

To explore this question, we conducted additional experiments by taking the molar ratio of NaCl to 10 and 30, respectively. We sampled, quenched, washed, filtered, dried and tested two materials with different salt contents when heated to 700°C and when heated to 800°C and held for 2h, respectively. Their XRD patterns and SEM images are shown in Figure S9 and Figure S10.

The unique Na-birnessite intermediate appears in two samples with two different NaCl contents at 700-0h, and it is a predominantly present phase. However, in XRD and SEM, Na-birnessite largely disappears from the 800-2h sample. This is consistent with the experimental phenomena which NaCl molar ratio is 20, indicating that the NaCl content does not affect the growth mechanism of NMO.



**Figure S9. XRD patterns and SEM images of samples with NaCl molar ratio of 10 for 700-0h and 800-2h**

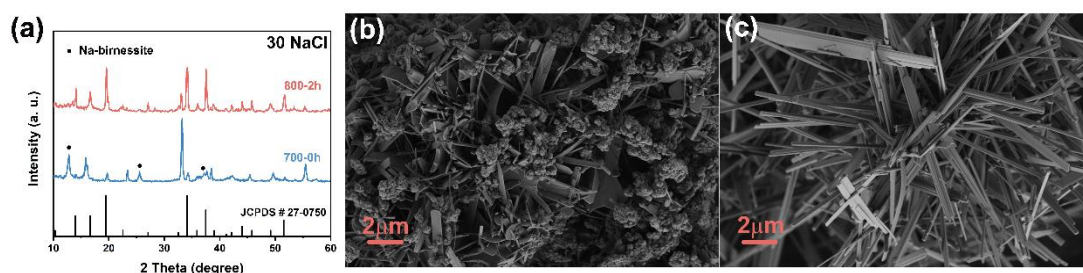


**Figure S10. XRD patterns and SEM images of samples with NaCl molar ratio of 30 for 700-0h and 800-2h**

**Table S1. Summary of Na<sub>0.44</sub>MnO<sub>2</sub> prepared by different methods as cathodes of SIB**

Method	Calcination temperature and time	Capacity retention rate	Rate capability	Ref.
Oxalate precursor method	900°C for 3 h	86% after 500 cycles (20 C)	90 mAh g <sup>-1</sup> (5 C)	3
Ultrasonic sonochemical method	900°C for 2 h	95% after 55 cycles (0.1 C)	61 mAh g <sup>-1</sup> (1 C)	4
Polymer-pyrolysis method	750°C for 24 h	77% after 1000 cycles (0.5 C)	82 mAh g <sup>-1</sup> (2 C)	5
Solid phase method	900°C for 15 h	86% after 600 cycles (5 C)	-	1
Electrospinning method	900°C for 9 h	89% after 3300 cycles (5 C)	31.7 mAh g <sup>-1</sup> (50 C)	6
Solution combustion method	800°C for 12 h	~97% after 250 cycles (4 C)	103 mAh g <sup>-1</sup> (4 C)	7
Reverse microemulsion method	850°C for 20 h	99.6% after 2000 cycles (8.3 C)	54.7 mAh g <sup>-1</sup> (10 C)	8
Sol-gel method	900°C for 15 h	100% after 100 cycles (0.1 C)	>120 mAh g <sup>-1</sup> (0.1 C)	9
Hydrothermal method	205°C for 96 h	~100% after 30 cycles (0.2 C)	90 mAh g <sup>-1</sup> (0.2 C)	10
Molten salt method	850°C for 5 h	94% after 40 cycles (0.5 C)	76 mAh g <sup>-1</sup> (2 C)	11
Molten salt method	800°C for 2 h	85.4% after 500 cycles (1 C)	65.3 mAh g <sup>-1</sup> (20 C)	This work

**Table S2. Elemental Analysis Results of NMO-8002 ICP-OES**

	Mass ratio	Atomic ratio
Na	9.7172	0.42
Mn	54.9896	1

## References

- 1 M. S. Chae, H. J. Kim, H. Bu, J. Lyoo, R. Attias, B. Dlugatch, M. Oliei, Y. Gofer, S. T. Hong and D. Aurbach, The Sodium Storage Mechanism in Tunnel-Type  $\text{Na}_{0.44}\text{MnO}_2$  Cathodes and the Way to Ensure Their Durable Operation, *Adv. Energy Mater.*, 2020, **10**, 2000564.
- 2 Z. Zhao, X. Huang, Y. Shao, S. Xu, L. Chen, L. Shi, Q. Yi, C. Shang and D. Zhang, Surface modification of  $\text{Na}_{0.44}\text{MnO}_2$  via a nonaqueous solution-assisted coating for ultra-Stable and High-Rate sodium-ion batteries, *Chem. Eng. J. Adv.*, 2022, **10**, 100292.
- 3 D. Zhang, W.-j. Shi, Y.-w. Yan, S.-d. Xu, L. Chen, X.-m. Wang and S.-b. Liu, Fast and scalable synthesis of durable  $\text{Na}_{0.44}\text{MnO}_2$  cathode material via an oxalate precursor method for Na-ion batteries, *Electrochim. Acta*, 2017, **258**, 1035.
- 4 G. S. Shinde, P. D. Nayak, S. P. Vanam, S. K. Jain, A. D. Pathak, S. Sanyal, J. Balachandran and P. Barpanda, Ultrasonic sonochemical synthesis of  $\text{Na}_{0.44}\text{MnO}_2$  insertion material for sodium-ion batteries, *J. Power Sources*, 2019, **416**, 50.
- 5 Y. Cao, L. Xiao, W. Wang, D. Choi, Z. Nie, J. Yu, L. V. Saraf, Z. Yang and J. Liu, Reversible sodium ion insertion in single crystalline manganese oxide nanowires with long cycle life, *Adv Mater*, 2011, **23**, 3155.
- 6 Y. Liu, X. Liu, F. Bu, X. Zhao, L. Wang, Q. Shen, J. Zhang, N. Zhang, L. Jiao and L.-Z. Fan, Boosting fast and durable sodium-ion storage by tailoring well-shaped  $\text{Na}_{0.44}\text{MnO}_2$  nanowires cathode, *Electrochim. Acta*, 2019, **313**, 122.
- 7 N. Sheng, C.-g. Han, Y. Lei and C. Zhu, Controlled synthesis of  $\text{Na}_{0.44}\text{MnO}_2$  cathode material for sodium ion batteries with superior performance through urea-based solution combustion synthesis, *Electrochim. Acta*, 2018, **283**, 1560.
- 8 Q. Liu, Z. Hu, M. Chen, Q. Gu, Y. Dou, Z. Sun, S. Chou and S. X. Dou, Multiangular Rod-Shaped  $\text{Na}_{0.44}\text{MnO}_2$  as Cathode Materials with High Rate and Long Life for Sodium-Ion Batteries, *ACS Appl Mater Interfaces*, 2017, **9**, 3644.
- 9 M. Xu, Y. Niu, C. Chen, J. Song, S. Bao and C. M. Li, Synthesis and application of ultra-long  $\text{Na}_{0.44}\text{MnO}_2$  submicron slabs as a cathode material for Na-ion batteries, *RSC Adv.*, 2014, **4**, 38140.
- 10 A. T. Ta, V. N. Nguyen, T. T. O. Nguyen, H. C. Le, D. T. Le, T. C. Dang, M. T. Man, S. H. Nguyen and D. L. Pham, Hydrothermal synthesis of  $\text{Na}_4\text{Mn}_3\text{O}_{18}$  nanowires for sodium ion batteries, *Ceram. Int.*, 2019, **45**, 17023.
- 11 L. Zhao, J. Ni, H. Wang and L. Gao, FLUX SYNTHESIS OF  $\text{Na}_{0.44}\text{MnO}_2$  NANORIBBONS AND THEIR ELECTROCHEMICAL PROPERTIES FOR Na-ION BATTERIES, *Funct. Mater. Lett.*, 2013, **06**, 1350012.